

<https://doi.org/10.1590/2318-0331.272220210107>

Meteorological-hydrodynamic model coupling for safe inland navigation of waterway stretches in dam reservoirs, using a scarce database

Modelo de acoplamento meteorológico-hidrodinâmico para navegação interior segura em trechos de hidrovias em reservatórios de barragens, usando um banco de dados escasso

Germano de Oliveira Mattosinho¹ , Geraldo de Freitas Maciel² , Fabiana de Oliveira Ferreira³ ,
Adriana Silveira Vieira⁴  & Yuri Taglieri São² 

¹Instituto Federal de Educação, Ciência e Tecnologia de Minas Gerais, Piumhi, MG, Brasil

²Faculdade de Engenharia de Ilha Solteira, Universidade Estadual Paulista, Ilha Solteira, SP, Brasil

³Universidade Federal de Mato Grosso, Cuiabá, MT, Brasil

⁴Universidade Estadual de Mato Grosso do Sul, Coxim, MS, Brasil

E-mails: germano.mattosinho@ifmg.edu.br (GOM), geraldo.f.maciel@unesp.br (GFM), fabiana.ferreira1@ufmt.br (FOF), adriana.vieira@uems.br (ASV), yuri.sao@unesp.br (YTS)

Received: August 13, 2021 - Revised: October 28, 2021 - Accepted: November 27, 2021

ABSTRACT

The SWAN (Simulating WAVes Nearshore) numerical model has been used and validated in numerous studies of open coastal and estuarine regions. Its application on inland or restricted waters (dam reservoir) is not only innovative and challenging, but also an important scientific contribution, filling a gap in the literature. We analyze the performance of the SWAN in the characterization of the agitation caused by the action of wind waves in the reservoir of the Ilha Solteira dam, considering measured wind velocities and a complex bathymetry. The studied area is close to a segment of the Tietê-Paraná waterway, in Brazil. Wind conditions were obtained by a 2D sonic anemometer installed in the reservoir during one of the measurement campaigns, for a period of 3 months. The estimates of the amplitude of waves generated in the reservoir were compared with measurements of the free surface elevation obtained by a Druck pressure sensor installed in the reservoir of the dam, about 300 m from the margin (already in intermediate/deep waters), and 1.0 m deep. The results obtained (amplitudes and wave periods) were shown to be promising and, albeit with significant heights overestimated, could be used for engineering preliminary drafts.

Keywords: Dam reservoirs; Field data; SWAN model; Waterway; Wind waves.

RESUMO

O modelo numérico SWAN (Simulating WAVes Nearshore) tem sido usado e validado em vários estudos de regiões costeiras abertas e estuarinas. Sua aplicação em águas interiores ou restritas (reservatório de barragens) não é apenas inovadora e desafiadora, mas também uma importante contribuição científica, preenchendo uma lacuna na literatura. Analisamos o desempenho do SWAN na caracterização da agitação causada pela ação das ondas geradas pelo vento no reservatório da barragem de Ilha Solteira, considerando velocidades de vento medidas e uma complexa batimetria. A área estudada está próxima a um trecho da hidrovia Tietê-Paraná, no Brasil. As condições do vento foram obtidas por um anemômetro sônico 2D instalado no reservatório durante uma das campanhas de medição, por um período de 3 meses. As estimativas da amplitude das ondas geradas no reservatório foram comparadas com as medidas da elevação da superfície livre obtidas por um sensor de pressão Druck instalado no reservatório da barragem, a cerca de 300 m da margem (já em águas intermediárias/profundas), e a 1,0 m de profundidade. Os resultados obtidos (amplitudes e períodos de onda) mostraram-se promissores e, com alturas significativas superestimadas, poderiam ser utilizados em nível de anteprojetos de engenharia.

Palavras-chave: Reservatórios de barragens; Dados de campo; Modelo SWAN; Hidrovia; Ondas geradas pelo vento.



INTRODUCTION

Studies on the generation and the propagation of waves produced by the action of wind have been carried out successfully for open coastal areas (Ou et al., 2002, Gonçalves et al., 2014, Hoque et al., 2020, Xu et al., 2020). Such studies have been validated by confrontation of numerical results and empirical data obtained by buoys located offshore and on the coast. On the other hand, the analysis of generation and propagation of wind waves in large water bodies, such as dam reservoirs, is less explored by the literature. In Brazil, these reservoirs are generally connected to waterways and allow inland navigation, turning the analysis of wind waves relevant to avoid accidents that can damage the vessels and/or hinder the flow of cargo on commercial routes.

The safety of inland navigation and the mitigation of significant erosive phenomena in lacustrine environments require a precise estimate of the action of wind waves (wave forces) on the reservoir margins and on structures, whether they are fixed (such as dams, containment walls, docking structures and guide walls) or mobile (like the vessel itself). For these reasons, it has become increasingly important to develop methodologies and tools capable of promoting the forecasting and monitoring of wind waves in reservoirs and stretches of waterways. In this sense, the control over the reservoir's free surface agitation level and its effects on fixed or mobile structures and on the margins is indeed an essential element in the construction of a basis for a future alert system (Diebold & Heller, 2017; Marques & Andrade, 2017; Mattosinho et al., 2018; Różyński, 2018; Jalil et al., 2019; Li et al., 2019; Mattosinho et al., 2019; Holanda et al., 2020).

In order to develop such methodologies and tools, numerical models are very useful to evaluate wind waves generation and forecasting. One of the most employed tools for estimating waves is the SWAN (Simulating Waves Nearshore) model proposed by Booij et al (1996, 1999), which is capable to simulate the generation, propagation and dissipation of the agitation in coastal regions and inland waters, based on the wind kinetics and on the wave action conservation equation. Although very useful, numerical models such SWAN require validation and calibration using empirical data, e.g. measurement stations (buoys). In this context, van Gruijthuijsen (1996) presented a validation of the SWAN model using field data from Lake George, Australia. Such lake is considered shallow, with a practically constant depth of 2.0 m. Using empirical results from eight buoys along the longest axis (north-south) of the lake and three case studies with constant wind velocities (stationary state), van Gruijthuijsen (1996) made evident the applicability of the SWAN model on restricted waters, evaluating and calibrating distinct parameters and formulations.

Along these lines, Jin & Ji (2001) also employed the SWAN model in the shallow waters of the Lake Okeechobee (average depth of 3,0 m), using two sets of wind and wave height data: 1) a 6-day data from 1989 for model calibration; and 2) a 6-day data from 1996 for model validation. The analyses showed a good agreement between the measured and the simulated data and a strong correlation between wave height and wind stress. The SWAN model was also used by Moeini & Etemad-Shahidi (2009) to analyze wind waves in Lake Erie, North America. The researchers considered the wind dynamics and a complex bathymetry varying up to 58 m deep, with an average depth of

19 m. The study data was collected for 276 h, for eleven and a half days. Among the main results, researchers point out that SWAN model showed good capacity in predicting the variations of H_s (significant wave height) and T_p (peak period) when wind suddenly changes direction and velocity. Mao et al. (2016) used a 10-year database of wind velocity and significant wave height to verify the sensitivity of equations and parameters of the SWAN model using unstructured meshes and subsequently calibrate it. A good agreement between numerical and field data was found.

While the SWAN model has been widely applied in open, estuarine and semi-confined areas, its application in closed areas (dam reservoirs) is less explored by the literature and, specifically in Brazil, is almost nonexistent. In this context, the ONDISA Project, led by the São Paulo State University (UNESP) (Trovati, 2001), designed a pilot venture focused on measurement campaigns aiming to infer about the hydrodynamics of the wind waves in the Ilha Solteira HPP (Hydroelectric Power Plant) reservoir, part of the important Tietê-Paraná Waterway. The acquisition of field data, its processing, treatment and analysis, together with the numerical modeling allowed for globally identifying, for the first time, the local wave climate and its actions on the surroundings.

Given the relevant role of the Tietê-Paraná Waterway in the economy and sustainability, this work carried out a field research in the reservoir of the HPP Ilha Solteira Dam, which contains a segment of the navigation route of the Tietê-Paraná Waterway running upstream. An observation cell gathered located 300 m away from the left bank's margins of the reservoir gathered data from January to March 2011. Within the scope of the ONDISA Project, this work confronts significant wave height and wave period from field measurement with numerical simulations obtained through SWAN.

In this sense, this work contributes to the literature by applying the SWAN model in the Ilha Solteira HPP reservoir, using local wind data (velocity, direction) and complex local bathymetry as input information for the model to compare numerical results with scarce field data (measurements from January to March) and guide future work. Such contribution is important since there is a lack of studies considering complex bathymetry and wind dynamics on reservoirs in Brazil; for Ilha Solteira HPP reservoir, for example, there are no application of any numerical models taking into account both aspects, despite being part of an important commercial route in Mercosul. Details of the field experiments, the wind and wave implementation and monitoring, along with the numerical simulations within the SWAN code can be found in Sections "Field measurement" and "Mathematical modelling and numerical methods employed by SWAN".

DESCRIPTION OF THE STUDY SITE

The Ilha Solteira Dam reservoir is part of the Urubupungá Complex, the sixth largest hydroelectric complex in the world, located 5 km away from the city of Ilha Solteira, a Brazilian municipality that belongs to the Northwest region of the State of São Paulo.

In terms of climatology, the lake is classified by the Kopen type Aw as a savanna climate (summer rains), with moderate winds (less than 10 m/s), occasional storms, and high magnitude gusts, with winds reaching 47.5 m/s (170 km/h), such as those recorded

in 2010 (Hernandez, 2010). The prevailing winds are derived from the Northeast, which, acting over a track on the order of tens of kilometers, can produce waves of 1.5 m along the navigation route, under extreme situations (Vieira, 2013).

The Ilha Solteira Dam reservoir is located at latitude $20^{\circ}25'58''$ south, longitude $51^{\circ}20'33''$ west, at an altitude of approximately 335 m. Such location, close to the confluence of the Tietê and Paraná rivers and the border with the State of Mato Grosso do Sul, makes the Ilha Solteira Dam reservoir a significant study cell for the important Tietê-Paraná waterway (Figure 1), and a vital segment of the Mercosul's commercial route.

The Tietê-Paraná Waterway is an extremely important navigation route connecting the producing regions of the Brazilian Cerrado (states of Mato Grosso, Mato Grosso do Sul, Goiás, and part of Rondônia, Tocantins and Minas Gerais) and the railway system leading to the Port of Santos. This waterway includes reservoirs of large-sized, multiple-use dams, especially the Ilha Solteira Dam reservoir. Due to its large dimension and length of the fetch (over 12.5 km in accordance with Marques et al., 2007), wind waves can cause problems regarding the navigation safety, the stability of the reservoir margins (erosion due to the impact of waves) and the local infrastructure (moorings).

In fact, accidents with inland waterway vessels, especially in lakes or in stretches of waterways in dam reservoirs, have been frequent, with significant economic and environmental losses (G1, 2013). Among the accidents reported in Brazilian Navy bulletins, the collision of convoys on bridges and tower structures have been the most frequent. These accidents result in serious damage, to the point of causing interdictions on heavy traffic highways. On October 17th, 2010, winds of 170 km/h in Ilha Solteira (northwest of the state of São Paulo) brought down nine transmission towers of the Ilha Solteira Hydroelectric Plant into the waters of the Paraná River. The fall affected 4 of the 6 transmission lines, making it impossible for the plant to fully generate energy and forcing it to open its spillways to maintain the system (Hernandez, 2010). Significant wave heights of 1.5 m were estimated in the reservoir (Vieira, 2013).

In 2013, a barge owned by the ADM / Sartco company, sailing the Tietê-Paraná Waterway in the Araçatuba region, between the Nova Avanhandava dam and the Três Irmãos reservoir, collided with a transmission tower from the Paulista Electricity Transmission Company (CTEEP), causing damage in two more towers on the riverbed and other three on land. According to shipping companies, this accident generated a loss of more than R\$ 12 million, since approximately a hundred thousand tons of

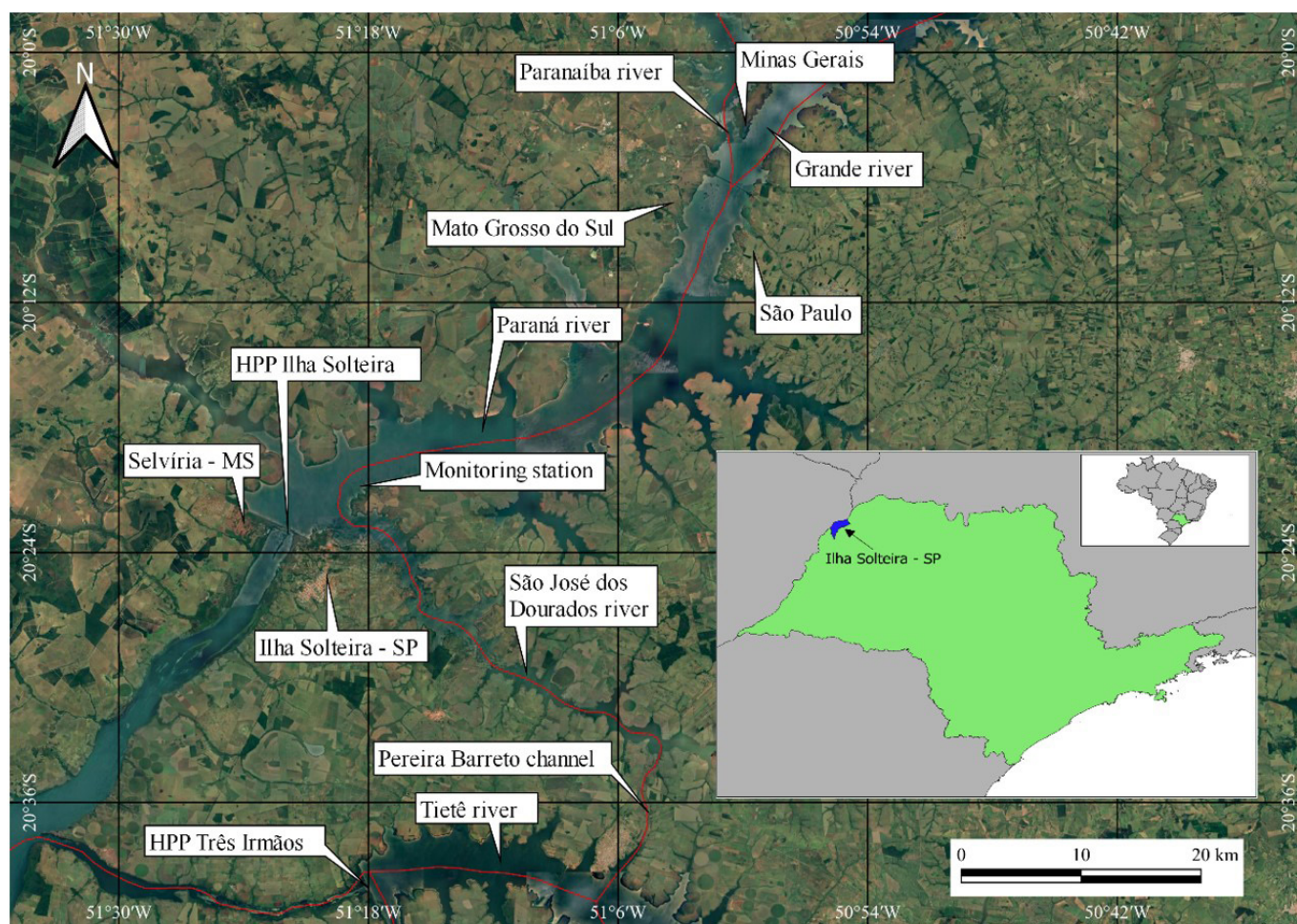


Figure 1. Stretch of the Tietê-Paraná waterway, monitoring station in the dam reservoir of HPP Ilha Solteira, name of the rivers, states and interest locals. The red line is the waterway route. (geocentric reference: SIRGAS 2000/UTM ZONE 22S – EPSG:4618).

soybeans were not transported during the eight days the waterway was closed (Vieira, 2013). Accidents of this nature have also been recorded in the Mississippi River waterways (G1, 2011) and in segments of the Rhine River in Europe (Reuters, 2011).

From the modern perspective of sustainability and in the face of climate change, inland navigation, especially in the case of the Tietê-Paraná waterway, became a fundamental link for the Brazilian economy since waterway transport is effectively an option to mitigate gas emissions responsible for the greenhouse effect. Notwithstanding, this mode of transport should be significantly expanded in the next two decades (Stamm, 2020).

FIELD MEASUREMENT

The equipment (pressure sensors, anemometers, etc.) were installed in a tree inside the Ilha Solteira reservoir, located at 20°20'49.07" latitude, and 51°18'17.63" longitude. Wind velocity and direction were measured by a 2D sonic anemometer positioned 1.2 m above the water level; its values were corrected using a standard height of 10 m (U_{10}). The data were stored in a datalogger and then transmitted to a database by telemetry. Pressure data, or pressure spectrum, was acquired by a Druck PDCR 1830 pressure sensor (for up to 50 psig, 0.06% non-linearity of the full scale, equipped with a 150 m cable feed) positioned 1.0 m below the water level (a ventilation tube provided the reference atmospheric pressure). Then, the pressure spectrum was converted into elevation data using the Linear Wave Theory, applying the appropriate pressure coefficient k_p (Ancil & Quach, 1997, Vieira, 2013), and wave properties were determined, such as height and period. Pressure fluctuations associated to the passing of the waves are rapidly attenuated because of the depth. Due to the frequencies, the immersion depth and the total local depth, the pressure sensor was positioned by experienced operators. Additionally, the field data resulted from a measurement station located in deep/intermediate waters, a suitable condition for Linear Theory (Ancil & Quach, 1997). According to Vieira (2013), this reasoning is also shared by the National Institute of Oceanography, England.

The main aspects to adequately acquire field data were data sampling frequency and transmission velocity by radio waves. Since both height and period of the waves were not previously known, an almost continuous sampling was chosen, along with the highest possible transmission velocity. Field data were registered using a CR 1000 datalogger, which had an internal program that constantly checked its available memory and the required transmission time so that the available memory was never full. As the datalogger available memory is dependent on the frequency at which data were transmitted, the transmission was adjusted to be carried out every hour. In a potential communication failure, the transmission would occur at every 30 minutes; if such failure remains, transmission interval would decrease to 10 minutes and to every minute, as a last resort. Furthermore, additional time was considered as a safety factor to avoid possible data loss due to transmission problems. 112,801 wind velocity minute-by-minute data were acquired in this procedure.

Therefore, based on the first tests, a frequency of 8 Hz was adopted for the pressure sensor, and of 0.2 Hz for the anemometer. Due to the topography and the distance of the main laboratory,

the UNESP Hydrology and Hydrometry Laboratory (LH²), data was transmitted to a repeater tower located at a higher altitude and then retransmitted to UNESP's LH².

Bathymetry data was obtained through an echo sounder (Navisound 205) with 0.1 m of resolution, which emits sound waves in a pre-established frequency and recaptures them after reaching an obstacle. The distance is calculated by using the wave emitting-returning time interval and the previously known wave velocity. To obtain georeferenced coordinates, the echo sounder was coupled to a computer-integrated GPS system (disregarding reservoir level variation).

MATHEMATICAL MODELLING AND NUMERICAL METHODS EMPLOYED BY SWAN

Bathymetric data were acquired and processed in the ONDISA Project (Trovati, 2001). From the available data, meshes were created using Portable Aquaveo SMS 10 software and coordinate data were exported to an electronic spreadsheet. Using x- and y- coordinates, the reservoir contour file was created and the initial points of the georeferenced mesh were checked. Finally, using the z-ordinate, the file "bottom.bot" (bathymetry) was created to be inserted in the SWAN model.

SWAN is an open-source numerical model developed at the Delft University of Technology (TUDelft), in Netherlands. The main goal of the SWAN model is to solve the spectral action balance equation without any a priori restrictions on the spectrum for the evolution of wave growth (third-generation wave model) (Booij et al., 1996, The SWAN Team, 2020a). The SWAN model is based on the wave action balance equation with sources and sinks, the shallow water wave model SWAN is an extension of the deep water third-generation wave models and the basic scientific philosophy of SWAN is identical to that of classic model WAM cycle 3 (The SWAN Team, 2020b).

SWAN model is used for obtaining realistic estimates of wave parameters in coastal areas, lakes and estuaries from given wind, bottom and current conditions, i.e. in any body of water which wind waves are relevant. Application in closed areas, such as lakes and dam reservoirs, can be found in van Gruijthuijsen (1996), Jin & Ji (2001), Moeini & Etemad-Shahidi (2009), Maciel et al., (2012), Vieira (2013) and Vieira et al. (2014).

The model uses the wind characteristics of a defined region (velocity, direction and frequency, in permanent or non-permanent regime), to simulate the wave height using a pre-established bathymetry data and propagate waves into the entire computational domain from predetermined wave records measured in some specific boundaries of the domain.

The equations solved with the SWAN, by finite difference method, refer to wave generation, dissipation and non-linear interaction in deep, intermediate and shallow waters. In this study, the time-step used was 1 minute and the iteration process runs until 50 iteration or when 97% of accuracy was reached between two subsequent iterations considering significant wave height (The SWAN Team, 2020b).

Table 1 presents the relevance of each physical process in the wave mechanics for each depth condition, i.e. deep water, intermediate water and shallow water (Beji & Battjes, 1994).

The spectrum action balance equation is a function of the action density, $N(\sigma, \theta) = E(\sigma, \theta) / \sigma$, where σ is the relative frequency, θ is the direction of the wave and E is the energy density. Formulated in Eulerian coordinates, the equation of the spectrum action balance is given by Equation 1:

$$\frac{\partial N}{\partial t} + \frac{\partial c_x N}{\partial x} + \frac{\partial c_y N}{\partial y} + \frac{\partial c_\theta N}{\partial \theta} + \frac{\partial c_\sigma N}{\partial \sigma} = \frac{S_{tot}(\sigma, \theta)}{\sigma} \quad (1)$$

The first term on the left side of Equation 1 represents the local rate of change of action density over time. The second and third terms respectively represent the propagation of the action density in the horizontal plane $x - y$, with the wave group velocity in space $c(x, y, \theta, \sigma)$. The fourth term represent the change in the relative frequency due to variations in depths and currents. Lastly, the fifth term depicts the refraction induced by depth and current. In summary, the left side of Equation 1 represents the model's kinematic portion, while the right side, the source term. From the right side of equation 1, S_{tot} is expressed by Equation 2.

$$S_{tot} = S_{in} + S_{nl3} + S_{nl4} + S_{ds,w} + S_{ds,b} + S_{ds,br} \quad (2)$$

These six terms for wave energy sources and sinks represent wave growth by wind input, nonlinear wave energy transfer through three-wave and four-wave interactions, wave decay due to whitecapping and bottom friction, and depth-induced wave breaking, respectively.

A rectangular grid with constant mesh sizes Δx and Δy in x- and y-direction, respectively, was chosen. The spectral space is divided into elementary bins with a constant directional resolution $\Delta \theta$ and a constant relative frequency resolution $\Delta \sigma / \sigma$ (resulting in a logarithmic frequency distribution). The velocity field does not depend on z . SWAN model was used in the default version without adding any new equations. Thus, the entire equations and discretization of the model can be verified in The SWAN Team (2020b).

SWAN's operation was carried out with the SOPRO platform, developed by LNEC – Laboratório Nacional de Engenharia Civil – (Fortes et al., 2006), in standard and non-stationary mode. The complete processing methodology, from data acquisition to SWAN results, is shown in Figure 2. Combination of three significant physical processes was considered in the simulations:

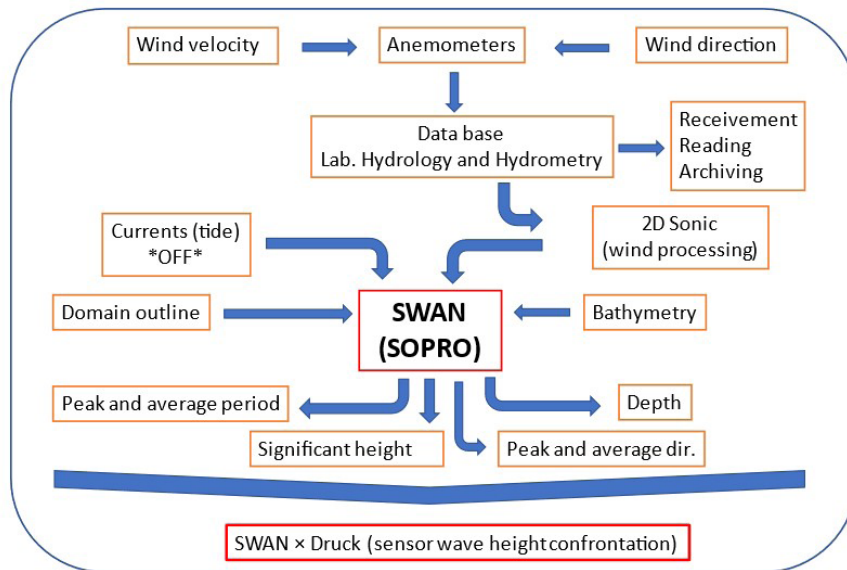


Figure 2. SWAN operation flowchart used.

Table 1. Important processes as the wave travels from deep to shallow waters. Adapted from Beji & Battjes (1994).

Processes	Deep water	Intermediate water	Shallow water
Wind generation	XXX	XXX	X
Quadruplet interactions	XXX	XXX	X
Triad interactions	O	O	XX
Partial breaking	O	XXX	X
Bottom friction	O	XX	XX
Refraction	X	X	XX
Shoaling	O	XX	XXX
Breaking	O	X	XXX
Reflection	O	O	X/XX
Diffraction	O	O	X

Symbols: Dominant (XXX); Significant (XX); Little Relevance (X) and Irrelevant (O).

wind generation, quadruplet interactions and bottom friction (as highlighted in Table 1). Each one of these physical processes has its own code input data, as shown in Table 2. Other physical processes were not explored due to the positioning of the measurement station in deep/intermediate waters.

The SOPRO platform is an intuitive graphical interface that assists in the creation of projects and automates operation to characterize the maritime agitation in each region. It unites several numerical models used by LNEC and is operated by Microsoft Access™, which has the advantage of having an integrated object-oriented programming language and driven by Visual Basic for Applications (VBA) events. One of the advantages of this language is the possibility of using and handling different Microsoft Windows applications (Fortes et al., 2006).

Figure 3 shows the bathymetry elevation data (Vieira, 2013) and the three two-dimensional rectangular computational domains used to produce three meshes with different grid resolutions. Boundary-fitted structured meshes in Cartesian coordinates were used. Mesh 1 consists of the coarser mesh and covers an area of 54 km x 33 km (rectangle 1 from Figure 3) using 1000 m x 1000 m size square cells. The intermediate mesh (Mesh 2) presents cell size of 500 m x 500 m and covers a 26.6 km x 18.4 km rectangle (rectangle 2 from Figure 3). Finally, Mesh 3 represents the refined mesh with cell size of 250 m x 250 m and covers a 14.8 km x

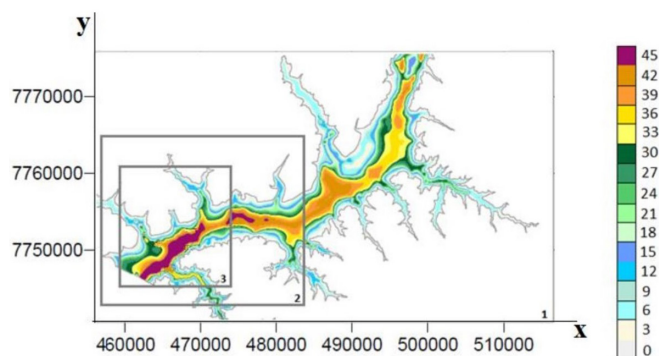


Figure 3. Bathymetry and domains in UTM coordinate for the SWAN model (Vieira, 2013). Rectangular domains are indicated with their respective number (1, 2 and 3).

Table 2. Input data in the SOPRO / SWAN platform (LNEC-Portugal, Fortes et al., 2006).

Wind (velocity, direction)	Data record (from Jan to Mar 2011)
Minimum Frequency for Waves (Hz)	0.05
Maximum Frequency for Waves (Hz)	3.00
Quadruple interactions	YES
Bottom friction	JONSWAP ($C_b = 0.067$)

Table 3. Summary of meshes characteristics. Meshes 1, 2 and 3 correspond to coarser, intermediate and refined meshes, respectively. X and Y are the origin of the rectangular domains. Δx and Δy are the cell size in each direction.

Mesh	X [UTM]	Y [UTM]	Number of Δx spacings	Number of Δy spacings	Δx (m)	Δy (m)
1	456680	7741700	58	33	1000	1000
2	457220	7744520	53	34	500	500
3	459329	7745690	58	57	250	250

14.3 km rectangle (rectangle 3 from Figure 3). Table 3 summarizes mesh and domains characteristics.

We used 3 meshes fitted with refinement to obtain greater accuracy of the simulated results at the point in question (monitoring station). Through the SOPRO platform, simulations using the finer mesh (Mesh 3) automatically employed the result of the intermediate mesh (Mesh 2) as boundary conditions and initial conditions in order to provide results in a reasonable computational time.

RESULTS

This section presents results from field measurements (wind and wave amplitudes) and numerical results of significant wave heights and average wave periods, along with statistical analysis to evaluate the code applicability. Figure 4 shows the wind data from January to March 2011 concerning mainly on wind direction and the distribution of wind velocity for each direction. The highest incidences of winds were coming from the NNE-ESE direction and it is observed that about 30% of the winds were ranging from 3.6 to 5.7 m/s. Data collected between 1977 and 1990 by the former São Paulo Energy Company (CESP) showed an average wind velocity of 3.0 m/s and NE as the predominant wind direction in the Ilha Solteira reservoir.

Figure 5 presents a more detailed wind data along with significant wave height data during the studied period (January to March 2011). Correlation coefficients of 0.74 and 0.95 were obtained from numerical/field data significant wave height comparison and wind velocity/SWAN significant wave height comparison, respectively.

Figure 6 compares the significant wave heights from field data with those estimated by SWAN. A correlation coefficient $R = 0.74$ is obtained along with p -value $\rightarrow 0$, indicating that an increase in the H_s of the pressure sensor results in an increase in the H_s of the SWAN and, moreover, suggests that the indicator R has statistical significance.

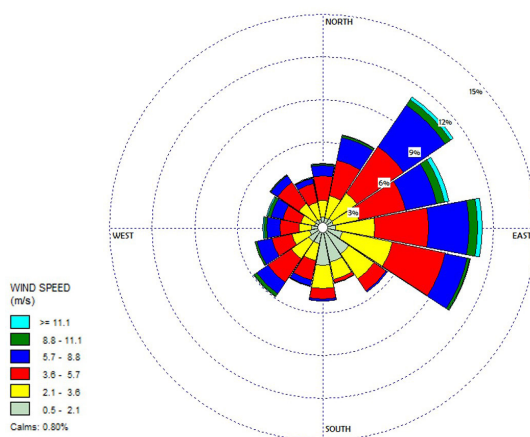


Figure 4. Wind rose from January to March 2011.

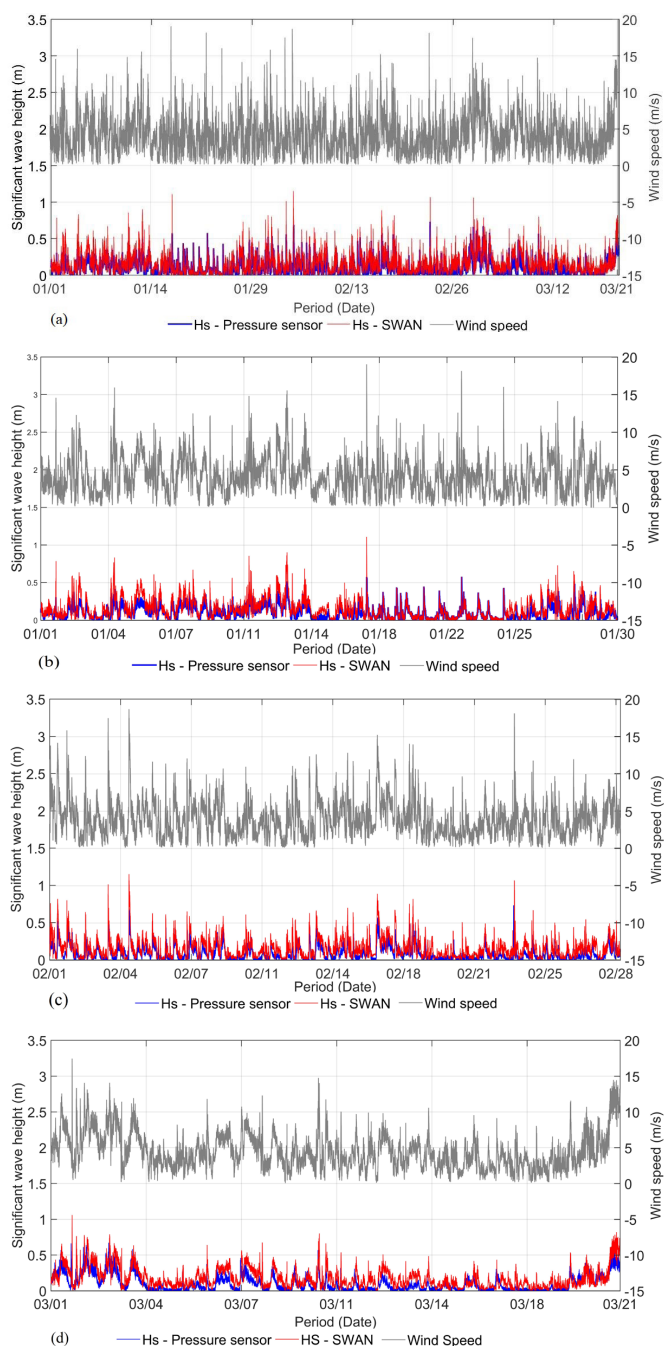


Figure 5. Analysis of the SWAN model, along with pressure sensor data of wind velocity and significant wave height from January to March 2011: (a) Total period, (b) Jan, (c) Feb, (d) Mar.

A qualitative result of significant wave heights and average wave periods is shown in Figure 7, using data from March 1, 2011 at 6:26 p.m., with winds registering an intensity of 13.1 m/s, coming from E-ENE (75.89 degrees). The SWAN model provided peak periods, T_p , varying from 0.5 s to 4.5 s versus $T_p = 2.0$ s to 3.5 s, registered in the pressure sensor. The mean period provided by the SWAN was $T_m = 2.0$ s (Figure 7). The analysis extracted from the confrontation of the numerical simulation and the field measurements allowed for the assessment of more significant statistical parameters (Willmott et al., 1985) (Table 4). A global

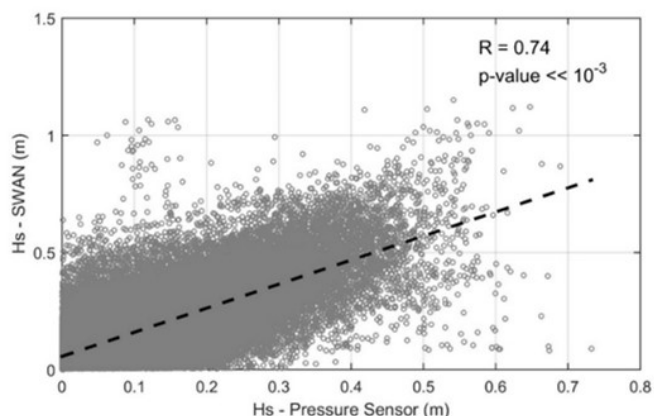


Figure 6. Scatter diagram of measured (H_s – Pressure sensor) and simulated (H_s – SWAN) significant wave heights.

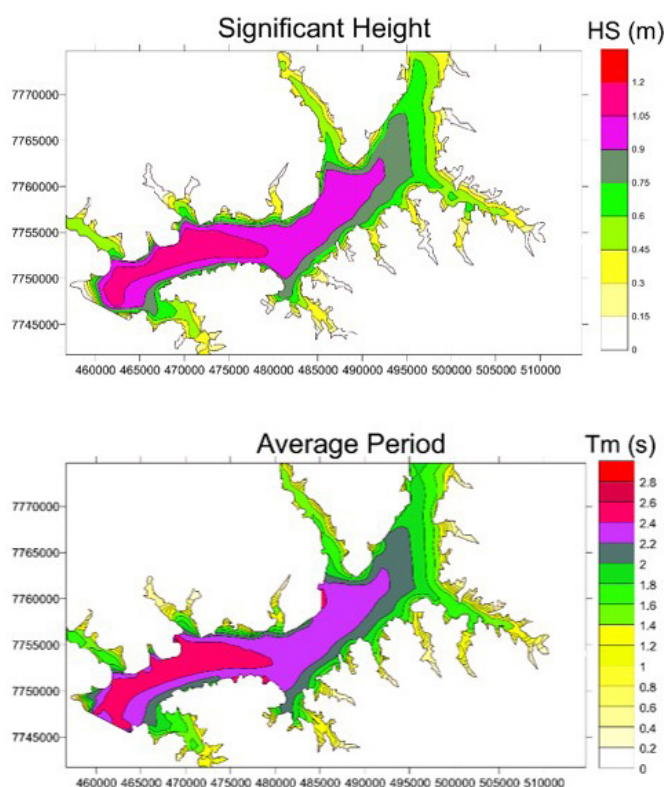


Figure 7. Graphical representation of significant wave heights and mean periods (Vicira, 2013).

analysis of these results showed an agreement index $IC = 76\%$ and a performance index (IP) in the order of 56%, even using a scarce database. This indicates an acceptability of forecasts and results considering the short period that the study was carried out.

DISCUSSIONS

As expected, higher velocities winds produce larger significant wave height, as shown in Figure 5. Such behavior and the forementioned correlation coefficients indicate that SWAN in

Table 4. Statistical data.

<i>H_s</i> (pressure sensor)	0.00 to 0.73 m
<i>RMSE</i>	0.11 m
<i>BIAS</i>	0.06 m
SWAN average	0.16 m
Pressure Sensor Average	0.10 m
<i>IC</i>	0.76
<i>R</i>	0.74
<i>IP = IC × R</i>	0.56

H_s: Significant wave height; *RMSE*: root-mean-square error; *IC*: concordance index; *R*: Pearson's correlation coefficient; *IP*: performance index.

fact produces physically coherent results in confined waters. The comparison between significant wave height and average wave period showed by Figure 7 reinforces the physical coherence of the code, as the regions with the highest significant wave heights are those with the highest mean periods, as expected and proven by the literature.

Despite the physical coherence showed by the code, a more detailed analysis indicates that SWAN code most of the time overestimated the significant heights of the waves (Figures 5 and 6), as well as in the work of Vieira et al. (2020). Further results from the literature show that SWAN applications can either underestimate or overestimate wave amplitude within the same data series when compared to measured data (Moeini & Etemad-Shahidi, 2009; van der Westhuysen, 2010; Gorrell et al., 2011; Pallares et al., 2014; Mao et al., 2016; Lemke et al., 2017; Kutupoğlu et al., 2018; Hoque et al., 2020) obtained through different media or equipment – buoys, pressure sensors, capacitance probes, non-intrusive sensors, etc.

In an analogous work to this, Moeini & Etemad-Shahidi (2009) also verified under and overestimating patterns of wave amplitudes, however also presenting good correlation with the field data ($R > 0.83$) with a mean *BIAS* of 0.02 m. Both correlation coefficient and mean *BIAS* presented by such work is in the same order of those statistical indicators obtained herein, indicating the applicability of the SWAN model in confined waters, e.g. dam reservoirs and lakes.

Although numerical simulations using SWAN present good agreement with field data (Figure 5) and their statistical indicators show agreement with literature (Moeini & Etemad-Shahidi, 2009; Mao et al., 2016), the action of complementary physical processes (Table 1) should be considered through more accurate verifications, since the experiment was conducted not only in deep waters also in intermediate waters and these processes might be dissipating spectrum energy. Indeed, the analysis of source term magnitudes in SWAN shows that, at greater water depths, whitecapping is the dominant dissipation term (De Waal, 2002; Bottema et al., 2003; Holthuijsen et al., 2008; Mao et al., 2016). In intermediate depths, the bottom friction becomes important, but it is surpassed in magnitude by the depth-induced breaking towards smaller dimensionless depths (van der Westhuysen, 2010).

The statistical results presented by Mao et al. (2016) for Lake Michigan after calibrating the model for the various buoys available in that work show that our results are within the range

observed, focusing mainly on the *BIAS* (0.028 - 0.601), *R* (0.51 - 0.96) and *RMSE* (0.10 - 0.39). Thus, despite not having our model calibrated for the case of Ilha Solteira, our data point to a good agreement between numerical results and field data.

However, degrees of underprediction for significant wave heights at two stations (45002 and 45007) in their work (-4.4% and -2.6%) are significantly larger than for wind velocity (-0.3% and -1.4%). Such difference may be originated from deficiencies in the treatment of deepwater wave physics (i.e., parametrization of whitecapping dissipation), since wind forcing is the primary driving agent of wave dynamics in an enclosed lake and underestimation of wave height can be partially attributed to wind velocity underprediction.

For dam lakes such as the Ilha Solteira HPP reservoir, there is no work with similar methodology for a direct confrontation. This work shows the applicability of the SWAN model for the case study, which can be improved after a new campaign to acquire wind velocity, wind-wave and bathymetry data using new methodological practices to acquire data and calibrate the model. Furthermore, the use of Fuzzy artificial neural networks to train the model is an aspect to be explored, as Santos et al. (2016) verified the potential of this tool.

CONCLUSIONS

This case study presents a temporal representation of wind and wave measurements in an observation site inside the Ilha Solteira HPP reservoir and confronts field data to numerical results using the SWAN code. Results from numerical simulations presented an agreement index of 76% and a performance index of 56% in comparison with field data. Such results corroborate another potentiality of the SWAN model in forecasting wind waves in closed areas, filling a gap concerning the applicability of the SWAN model in the prediction of wind waves in dam reservoirs, considering the wind dynamics and the complex bathymetry of deep/intermediate waters in transition zones.

The calculation code presented the expected agreement between mean period and significant wave height even using a scarce data-set, proving itself a useful tool in the prediction of risks for vessel traffic (critical zones) in reservoirs. Moreover, the methodology applied in this work can be used as data for preliminary projects, studies on protection of the margins, possible locations for implantation of tank-net systems (pisciculture), to assist in safe navigation through Tietê-Paraná waterway and to predict wave impact along the margins, contributing for determining the reservoir vulnerability index.

In view of the above, continuous studies and measurements are necessary to re-evaluate (explore) the numerical model. Further campaigns should use new technologies to perform additional bathymetry measurements, implement new methods for wave measurement, besides performing georeferencing and simultaneous wind × wave analysis (amplitudes, intensities, time duration, direction and periods). Notwithstanding, a detailed evaluation of the influence of each physical process on the Ilha Solteira reservoir should be carried out using at least 12 months of data and, as far as possible, at opposite points on each bank, along the waterbody, and especially on the navigation axis. Such

actions would constitute, in the first moment, conditions to design and implement an alert system at the service of waterway users in the axis navigation stretches within dam reservoirs.

ACKNOWLEDGEMENTS

To LNEC - National Laboratory of Civil Engineering of Portugal, for sharing the use of the SOPRO platform, in which the SWAN code is available. To the Federal Institute of Education, Science and Technology of Minas Gerais (IFMG) - Piumhi Advanced Campus for supporting the work developed. To FAPESP (processes 07/53029-5 and 02/11363-2) and FINEP (proc. CT-AQUA – FINEP 01.07.0784.00/2008) for financing part of the research. To members of the ONDISA Project for the shared data. To Professor Claudio Freitas Neves for his encouragement and participation in related projects.

REFERENCES

- Ancil, F., & Quach, T. T. (1997). Contrôle et analyse de mesures manométriques de vagues de surface. *Canadian Journal of Civil Engineering*, 24(4), 539-546. <https://doi.org/10.1139/196-120>.
- Beji, S., & Battjes, J. A. (1994). Numerical simulation of nonlinear wave propagation over a bar. *Coastal Engineering*, 23, 1-16. [https://doi.org/10.1016/0378-3839\(94\)90012-4](https://doi.org/10.1016/0378-3839(94)90012-4).
- Booij, N. R., Holthuijsen, L. H., & Ris, R. C. (1996). The SWAN wave model for shallow water. *Coastal Engineering*, 1, 668-676.
- Booij, N., Ris, R. C., & Holthuijsen, L. H. (1999). A third-generation wave model for coastal regions, part I: model description and validation. *Journal of Geophysical Research*, Hoboken, 104(C4), 7649-7666. <https://doi.org/10.1029/98JC02622>.
- Bottema, M., De Waal, J.P., Regeling, E.J. (2003). Some applications of the Lake IJssel/Lake Sloten wave data set. *Coastal Engineering*, 413-425. https://doi.org/10.1142/9789812791306_0036.
- De Waal, J.P. (2002). Wave growth limit in shallow water. *Ocean Wave Measurement and Analysis*. [https://doi.org/10.1061/40604\(273\)58](https://doi.org/10.1061/40604(273)58).
- Diebold, M., & Heller, P. (2017). Scaling wind fields to estimate extreme wave heights in mountainous lakes. *Journal of Applied Water Engineering and Research*, 7(1). <https://doi.org/10.1080/23249676.2017.1317294>.
- Fortes, C. J., Pinheiro, L., Santos, J. A., Neves, M. G., & Capitão, R. (2006). SOPRO – Pacote integrado de modelos de avaliação dos efeitos das ondas em portos. *Tecnologias da Água*, 1, 51-61.
- G1. (2011). *Choque de barcas fecha temporariamente trecho do rio Mississipi*. Retrieved in 2020, January 11, from <http://g1.globo.com/mundo/noticia/2011/05/choque-de-barcas-fecha-temporariamente-trecho-do-rio-mississipi.html>
- G1. (2013). *Acidente na hidrovía em Araçatuba, SP, prejudica escoamento de grãos*. Retrieved in 2020, June 22, from <http://g1.globo.com/sao-paulo/sao-jose-do-rio-preto-aracatuba/noticia/2013/03/acidente-na-hidrovía-em-aracatuba-sp-prejudica-escoamento-de-graos.html>
- Gonçalves, M., Martinho, P., & Soares, C. G. (2014). Assessment of wave energy in the Canary Islands. *Renewable Energy*, 68, 774-784. <https://doi.org/10.1016/j.renene.2014.03.017>.
- Gorrell, L., Raubenheimer, B., Elgar, S., & Guza, R. T. (2011). SWAN prediction of waves observed on shallow water onshore of complex bathymetry. *Coastal Engineering*, 58, 513-516.
- Hernandez, F. B. (2010, October 17). *Torres de transmissão de energia caem em Ilha Solteira - Vento forte causou a queda* [Vídeo]. Retrieved in 2020, June 22, from <https://www.youtube.com/watch?v=7aUYZA0XpQ>
- Holanda, F. S. R., Wanderley, L. L., Mendonça, B. S., Rocha, I. P., Santos, L. D. V., & Pedrotti, A. (2020). Formação de ondas e os processos erosivos nas margens do lago da UHE Xingó. *Revista Brasileira de Geografia Física*. 13(2), 887-903. <https://doi.org/10.26848/rbgf.v13.2.p887-902>.
- Holthuijsen, L.H., Zijlema, M., van der Ham, P.J. (2008). Wave physics in a tidal inlet. *Coastal Engineering*, 437-448. https://doi.org/10.1142/9789814277426_0037.
- Hoque, M. A., Perrie, W., & Solomon, S. M. (2020). Application of SWAN model for storm generated wave simulation in the Canadian Beaufort Sea. *Journal of Ocean Engineering and Science*, 5, 19-34. <https://doi.org/10.1016/j.joes.2019.07.003>.
- Jalil, A., Li, Y., Zhang, K., Gao, X., Wang, W., Khan, H. O. S., Pan, B., Ali, S., & Acharya, K. (2019). Wind-induced hydrodynamic changes impact on sediment resuspension for large, shallow Lake Taihu, China. *International Journal of Sediment Research*, 34(3), 205-215. <https://doi.org/10.1016/j.ijsrc.2018.11.003>.
- Jin, K. R., & Ji, Z. G. (2001). Calibration and verification of a spectral wind-wave model for Lake Okeechobee. *Ocean Engineering*, 82(5), 571-584. [https://doi.org/10.1016/S0029-8018\(00\)00009-3](https://doi.org/10.1016/S0029-8018(00)00009-3).
- Kutupoglu, V., Çakmak, R. E., Akpınar, A., & van Vledder, G. Ph. (2018). Setup and evaluation of a SWAN wind wave model for the Sea of Marmara. *Ocean Engineering*, 165, 450-464.
- Lemke, N., Fontoura, J. A. S., Calliari, L. J., Aguiar, D. F., & Simão, C. E. (2017). Comparative study between modeled (SWAN) and measured (waverider buoy) wave data em Patos Lagoon – RS, Brazil. *Pan-American Journal of Aquatic Sciences*, 12(1), 1-13.
- Li, J., Zang, J., Liu, S., Jia, W., & Chen, Q. (2019). Numerical investigation of wave propagation and transformation over a submerged reef. *Coastal Engineering Journal*, 61(3), 363-379. <https://doi.org/10.1080/21664250.2019.1609712>.

- Maciel, G. F., Vieira, A. S., Fortes, J. C., Cunha, E. F., Ferreira, F. O., & Fiorot, G. H. (2012). Aplicação do Modelo Numérico SWAN à Geração e Propagação de Ondas Geradas por Vento em Recintos Fechados. In *XXV Congresso Latinoamericano de Hidráulica*. San José, Costa Rica.
- Mao, M., van der Westhuysen, A. J., Xia, M., Schwab, D. J., & Chawla, A. (2016). Modeling wind waves from deep to shallow waters in Lake Michigan using unstructured SWAN. *Journal of Geophysical Research. Oceans*, *121*, 3836-3865.
- Marques, M., & Andrade, F. O. (2017). Automated computation of two-dimensional fetch fields: case study of the Salto Caxias reservoir in southern Brazil. *Lake and Reservoir Management*, *33*(1), 62-73. <https://doi.org/10.1080/10402381.2016.1264514>.
- Marques, M., Maciel, G. F., & Sobrinho, M. D. (2007). Estimation of the maximum wind fetches in Ilha Solteira, state of São Paulo, reservoir. *Acta Scientiarum Technology*, *29*(1), 79-84. <https://doi.org/10.4025/actascitechnol.v29i1.112>.
- Mattosinho, G. O., Maciel, G. F., & Vieira, A. S. (2019). The swan-veg model as a useful tool in the prediction of waves in dam reservoirs. *Brazilian Journal of Development*, *5*(7). <https://doi.org/10.34117/bjdv5n7-075>.
- Mattosinho, G. O., Vieira, A. S., Maciel, G. F., Rocha, G. E., & Tardivel, J. L. C. (2018). Dissipação de energia de ondas pela vegetação em recintos fechados. In *XXVIII Congresso Latinoamericano de Hidráulica*. Buenos Aires, Argentina. Retrieved in 2020, November 19, from https://www.ina.gov.ar/congreso_hidraulica/Congreso_libro/TC_TEMA_3.pdf
- Moeini, M., & Etemad-Shahidi, A. (2009). Wave parameter hindcasting in a lake using the SWAN Model. *Scientia Iranica*, *16*(2), 156-164. Retrieved in 2020, August 15, from http://scientiairanica.sharif.edu/article_3187.html
- Ou, S. H., Liau, J. M., Hsu, T. W., & Tzang, S. Y. (2002). Simulating typhoon waves by SWAN wave model in coastal waters of Taiwan. *Ocean Engineering*, *29*, 947-971. [https://doi.org/10.1016/S0029-8018\(01\)00049-X](https://doi.org/10.1016/S0029-8018(01)00049-X).
- Pallares, E., Sánchez-Arcilla, A., & Espino, M. (2014). Wave energy balance in wave models (SWAN) for semi-enclosed domains – application to the Catalan coast. *Continental Shelf Research*, *87*, 41-53.
- Reuters, B. (2011). *Remoção de navio com ácido do Reno deve levar dias*. Retrieved in 2020, November 11, from <http://br.reuters.com/article/worldNews/idBRSPE70D08020110114>
- Rózyński, G. (2018). Local wave energy dissipation and morphological beach characteristics along a northernmost segment of the polish coast. *Archives of Hydro-Engineering and Environmental Mechanics*, *65*(2), 91-108. <https://doi.org/10.1515/heem-2018-0007>.
- Santos, F. L., Reis, M. T., Fortes, C. J. E. M., Lotufo, A. D., Neves, D. R. C. B., Poseiro, P., & Maciel, G. F. (2016). Performance of a fuzzy ARTMAP artificial neural network in characterizing the wave regime at the Port of Sines (Portugal). *Journal of Coastal Research*, *32*(6), 1362-1373.
- Stamm, M. (2020). *Mato Grosso tem duas obras prioritárias no ministério da Infraestrutura para 2020*. Retrieved in 2020, August 18, from <https://www.sonoticias.com.br/politica/mato-grosso-tem-duas-obras-prioritarias-no-ministerio-da-infraestrutura-para-2020/>
- The SWAN Team. (2020a). *SWAN User Manual – SWAN Cycle III version 41.31A*. Delft: Delft University of Technology.
- The SWAN Team. (2020b). *Scientific and Technical Documentation – SWAN Cycle III version 41.31A*. Delft: Delft University of Technology.
- Trovati, L. R. (2001). *Produção de ondas induzidas pelo vento no lago de Ilha Solteira*. Ilha Solteira: FEIS. 61 p. Retrieved in 2020, February 2, from https://www.feis.unesp.br/Home/departamentos/engenhariacivil/hidrologialh/rel_final_ondisa1.pdf
- van der Westhuysen, A. J. (2010). Modeling of depth-induced wave breaking under finite depth wave growth conditions. *Journal of Geophysical Research*, *115*(C1), <https://doi.org/10.1029/2009JC005433>.
- van Gruijthuijsen, M. F. J. (1996). *Validation of the wave prediction model SWAN using field data from Lake George, Australia* (Master's thesis). Department Hydraulic Engineering, Faculty of Civil Engineering and Geosciences, Technische Universiteit Delft, Netherlands. Retrieved in 2020, March 8, from, [em:http://resolver.tudelft.nl/uuid:a8a1face-a0ef-4307-85cf-7931c92bb6eb](http://resolver.tudelft.nl/uuid:a8a1face-a0ef-4307-85cf-7931c92bb6eb)
- Vieira, A. S. (2013). *Análises, aplicações e validações – numérico/experimentais do modelo SWAN em áreas restritas e ao largo* (Tese de doutorado). Departamento de Engenharia Elétrica, Faculdade de Engenharia de Ilha Solteira, Universidade Estadual Paulista, São Paulo.
- Vieira, A. S., Gregorio, I. C., Fortes, C. J. E. M., Tomohiro, S., & Maciel, G. F. (2014). Application of the numerical model SWAN in locations with vegetation in the Tiete-Paraná waterway in Lake of Ilha Solteira's Dam – Brazil. In *2nd International Conference on Maritime Technology And Engineering*. Lisboa, Portugal. <https://doi.org/10.13140/RG.2.1.2125.5200>.
- Vieira, F., Cavalcante, G., & Campos, E. (2020). Analysis of wave climate and trends in a semi-enclosed basin (Persian Gulf) using a validated SWAN model. *Ocean Engineering*, *196*, <https://doi.org/10.1016/j.oceaneng.2019.106821>.
- Willmot, C. J., Ackleson, S. G., Davis, R. E., Feddema, J. J., Klink, K. M., Legates, D. R., O'Donnell, J., Rowe, C. M. (1985). Statistics for the evaluation and comparison of models. *Journal of Geophysical Research*, *90*(C5), 8995-9005, <https://doi.org/10.1029/JC090iC05p08995>.
- Xu, Y., Zhang, J., Xu, Y., Ying, W., Wang, Y. P., Che, Z., & Zhu, Y. (2020). Analysis of the spatial and temporal sensitivities of key parameters in the SWAN model: an example using Chan-hom

typhoon waves. *Estuarine, Coastal and Shelf Science*, 232, <https://doi.org/10.1016/j.ecss.2019.106489>.

Authors contributions

Germano de Oliveira Mattosinho: First author who contributed to literature review, performed the simulation tests and discussion of results, as well as writing and formatting of the article.

Geraldo de Freitas Maciel: Research coordinator, paper conception, analysis and completion of results and discussion.

Fabiana de Oliveira Ferreira: Literature review, Performed the statistical tests, writing and revision of the article.

Adriana Silveira Vieira: Performed the simulation tests and discussion of results.

Yuri Taglieri São: Discussion of results and proofreading the article.

Editor in-Chief: Adilson Pinheiro

Associated Editor: Fernando Mainardi Fan